Excess silica in omphacite and the formation of free silica in eclogite

H. W. DAY AND S. R. MULCAHY
Department of Geology, University of California, Davis, One Shields Avenue, Davis, CA 95616, USA
(day@geology.ucdavis.edu)

ABSTRACT   Silica lamellae in eclogitic clinopyroxene are widely interpreted as evidence of exsolution during decompression of eclogite. However, mechanisms other than exsolution might produce free silica, and the possible mechanisms depend in part on the nature and definition of excess silica. 'Excess' silica may occur in both stoichiometric and non-stoichiometric pyroxene. Although the issue has been debated, we show that all common definitions of excess silica in non-stoichiometric clinopyroxene are internally consistent, interchangeable, and therefore equivalent. The excess silica content of pyroxene is easily illustrated in a three-component, condensed composition space and may be plotted directly from a structural formula unit or recalculated end-members. In order to evaluate possible mechanisms for the formation of free silica in eclogite, we examined the net-transfer reactions in model eclogites using a Thompson reaction space. We show that there are at least three broad classes of reactions that release free silica in eclogite: (i) vacancy consumption in non-stoichiometric pyroxene; (ii) dissolution of Ti-phases in pyroxene or garnet; (iii) reactions between accessory phases and either pyroxene or garnet. We suggest that reliable interpretation of the significance of silica lamellae in natural clinopyroxene will require the evaluation not only of silica solubility, but also of titanium solubility, and the possible roles of accessory phases and inclusions on the balance of free silica.

Key words: eclogite; excess silica; omphacite; pyroxene; ultrahigh-pressure.

INTRODUCTION

The origin and interpretation of excess silica in omphacitic pyroxene have been controversial since Eskola (1921) first reported 'pseudojadeite molecule' $[(Ca, Mg)(Al, Fe)_2Si_4O_{12}]$ in analyses of natural pyroxene from Norwegian eclogites, and Kushiro (1969) inferred its presence in synthetic clinopyroxene. Excess silica and alumina associated with vacancies in the structural formula have been recognized in pyroxene from high- and ultrahigh-pressure rocks (Williams, 1932; O'Hara & Yoder, 1967; Sobolev *et al.*, 1968; Smith & Cheeney, 1980; Smyth, 1980; Wang *et al.*, 1993). Based in part on those observations, oriented inclusions of quartz or coesite in clinopyroxene have been widely interpreted as the result of exsolution of that excess silica from the host during decompression from high or ultrahigh pressure (Liou *et al.*, 1998; Dobrzhinetskaya *et al.*, 2002; Klemd, 2003; Zhang *et al.*, 2005). However, mechanisms other than exsolution might also yield free silica as quartz, coesite, or stishovite, and those mechanisms depend in part on the nature and definition of excess silica.

In order to evaluate the possible mechanisms by which free silica might form, a common understanding is needed of how excess silica may be defined and measured, and a clear view of the spectrum of reactions by which silica might be released in eclogite. Eventually, experimental confirmation and calibration of some key reactions will also be required.

The goals of this study were to provide an internally consistent overview and reconciliation of several definitions of excess silica and to examine the mechanisms by which free silica may form in eclogite. We show that 'excess' silica occurs in both stoichiometric and non-stoichiometric pyroxene and that all common definitions of excess silica in non-stoichiometric pyroxene are internally consistent, compatible, and therefore equivalent. We will also show that free silica may form in eclogite not only by consumption of vacancies in pyroxene, but also by dissolution of Ti-bearing minerals and reactions of garnet and clinopyroxene with accessory phases.

Our considerations are limited to processes that might form lamellae or other inclusions of silica polymorphs in true eclogite, which lacks plagioclase. Free silica formed by the breakdown of plagioclase in precursor rocks may be present in eclogite, but those processes are not considered here.

Because there has been some recent debate about how best to express the compositions of pyroxene (Katayama *et al.*, 2000; Tsai & Liou, 2000; Klemd, 2003; Zhang *et al.*, 2003; Page *et al.*, 2005), we begin by considering the nature of excess silica in natural and synthetic pyroxene.

PYROXENE COMPOSITION SPACE

The essential features of excess silica in omphacite can be illustrated in the simplified system CaO-MgO-Al_2O_3-SiO_2 (CMAS, Fig. 1). Although omphacite also contains other major elements such as iron and sodium, the substitutions of these elements can be described with exchange operators that have no effect on silica content (e.g. $Fe^{2+}Mg_{-1}$, $Fe^{3+}Al_{-1}$, $NaAlCa_{-1}Mg_{-1}$; Thompson, 1982). Consequently, it is convenient to consider model pyroxene compositions that can be described with only four independent components, and, for the purpose of understanding the silica balance, it is not necessary to treat directly important end-members such as jadeite.

Excess silica in pyroxene is closely linked to non-quadrilateral components such as aluminium. Calcium clinopyroxene accommodates aluminium by a coupled substitution, $AlAlMg_{-1}Si_{-1}$, yielding the calcium Tschermak component ($CaAl_2SiO_6$, CaTs; Table 1) (Tschermak, 1871; Doelter, 1883) or by a vacancy substitution mechanism leading to calcium Eskola component ($Ca_{0.5}AlSi_2O_6$, CaEs; Table 1) (Eskola, 1921). Aluminous clinopyroxene was synthesized in early experiments (Zvetkov, 1945; Segnit, 1953; Clark et al., 1962), and Hays (1966, 1967) demonstrated that pure $CaAl_2SiO_6$ has a stability field above ~1.2 GPa. Up to 20–30 mol.% of CaEs can be accommodated in Di-CaTs pyroxene (Wood & Henderson, 1978; Wood, 1979) but the pure compound apparently has no stability field.
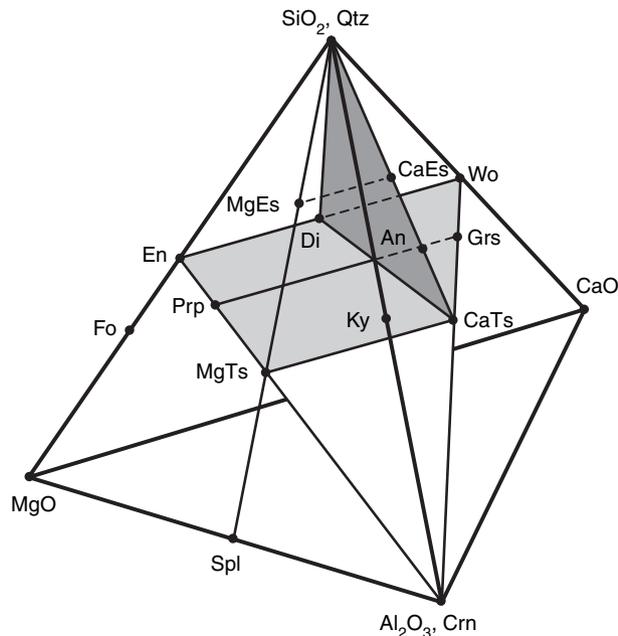
Fig. 1. Compositions in the system CaO-MgO-Al_2O_3-SiO_2 (CMAS). All formula units and abbreviations are listed in Table 1. The joins Di-CaTs, Prp-Grs, and MgTs-CaTs lie in the plane En-Wo-Crn.

Table 1. Formula units of end-members and components.

Name	Abbrev.	Formula
Anorthite	An	$CaAl_2Si_2O_8$
Ca Eskola pyroxene	CaEs	$Ca_{0.5}[\ ]_{0.5}AlSi_2O_6$
Ca Tschermak pyroxene	CaTs	$CaAl_2SiO_6$
Corundum	Crn	Al_2O_3
Diopside	Di	$CaMgSi_2O_6$
Enstatite	En	$Mg_2Si_2O_6$
Forsterite	Fo	Mg_2SiO_4
Geikielite	Gk	$MgTiO_3$
Grossular	Grs	$Ca_3Al_2Si_3O_{12}$
Jadeite	Jd	$NaAlSi_2O_6$
Kyanite	Ky	Al_2SiO_5
Mg Eskola pyroxene	MgEs	$Mg_{0.5}[\ ]_{0.5}AlSi_2O_6$
Mg Tschermak pyroxene	MgTs	$MgAl_2SiO_6$
Na-pyroxene	NaPx	$NaMg_{0.5}Si_{0.5}Si_2O_6$
Pyrope	Prp	$Mg_3Al_2Si_3O_{12}$
Quartz	Qtz	SiO_2
	3Qtz	Si_3O_6
Rutile	Rt	TiO_2
Spinel	Spl	$MgAl_2O_4$
Wollastonite	Wo	$Ca_2Si_2O_6$
Exchange components		
Jadeite exchange	jd	$NaAlCa_{-1}Mg_{-1}$
Mg-Ca exchange	mc	$MgCa_{-1}$
Tschermak exchange	tk	$Al_2Mg_{-1}Si_{-1}$
Ti-Si exchange	ts	$TiSi_{-1}$
Vacancy-Si exchange	vs	$[\ ]SiCa_{-1}Mg_{-1}$

In CMAS, stoichiometric pyroxene compositions lie in the En-Wo-Crn plane and contain four cations per six oxygen. Non-stoichiometric compositions with cation vacancies lie in the volume above that plane and necessarily contain more silica than stoichiometric pyroxene (Fig. 1). Consequently, four independent components are required in order to describe the observed range of pyroxene compositions. Excess silica in pyroxene compositions has commonly been expressed by using either CaEs or Qtz (Fig. 1) as a fourth component (e.g. Khanukhova et al., 1976a,b; Gayk et al., 1995; Tsai & Liou, 2000). In CMAS, the fourth component can conveniently be chosen to be Ky, Qtz, CaEs, MgEs, or even Fo or Spl (Fig. 1), but the sign of the fourth component and the calculated mole fractions of the remaining three components depend on that choice.

Regardless of the choice of components, any transformation of the coordinate system from the oxides to a structural formula or end-members must contain exactly equivalent information and the same number of independent components. Consequently, there is a direct relationship between structural formulae and any set of end-member components.

Figure 2a,b shows a new way to view the direct relationship between two commonly chosen end-member coordinate systems and the structural formula of clinopyroxene, which is used to clarify ambiguity about the definitions of excess silica. For purposes of illustration, it was assumed that clinopyroxene can be described in a degenerate three-component system, and all components, including silica, are written as six-oxygen formula units. It is convenient to use 3Qtz as a component because, as discussed below, isopleths of Si per formula unit (pfu) are parallel and the mole
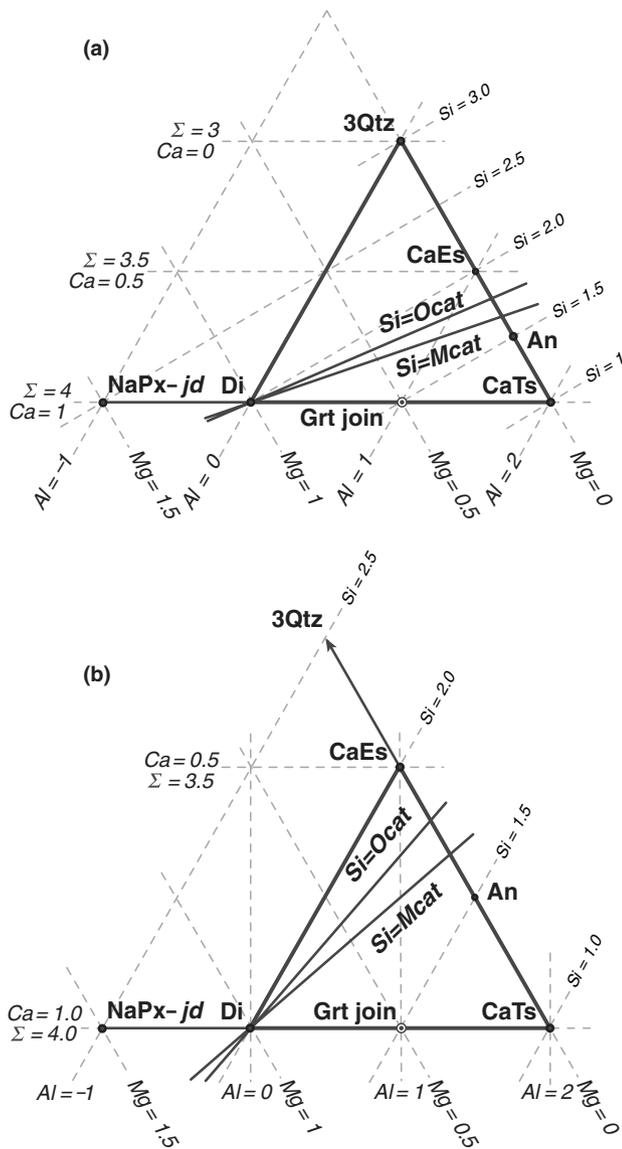
Fig. 2. Two coordinate systems for pyroxene compositions in CMAS. (a) Di-CaTs-3Qtz. (b) Di-CaTs-CaEs; abbreviations in Table 1. Dashed lines are contours of constant cation content and 'Σ' is total cations (per six-oxygen formula unit). The point labelled 'Grt join' marks the piercing point of the Prp-Grs join (Fig. 1). 'Ocat' is the sum of all cations excluding Si. 'Mcat' is the sum of M-site cations, excluding Si. The Si = Ocat line intersects the CaTs-3Qtz and CaTs-CaEs joins at $X_{CaTs} = 0.6$ and 0.2 respectively. The Si = Mcat line intersects these joins at $X_{CaTs} = 0.66$ and 0.33 respectively. See text for further discussion.

fraction of 3Qtz is numerically equal to the calculated cationic deficiency. The component 3Qtz (Si_3O_6) is identical to the component 'supersilipyx' defined by Smith (2006). In each of the coordinate systems, isopleths of constant Ca, Mg, Al and Si are parallel to lines of zero content of each cation. For example, isopleths of Si (pfu) are parallel to the Di-CaEs join in both coordinate systems because both end-members

contain two Si per six oxygen anions. Note that pyroxene below this join contains only ^{IV}Si whereas those above must also have some ^{VI}Si.

Contours of total cation content (Σ = total cations per six oxygen) are parallel to the Di-CaTs join in each coordinate system. Compositions above the Di-CaTs join have fewer than four cations, corresponding to vacancies in the structure. Although vacancies cannot be assigned to a particular site without additional assumptions, the contours of total cations are unique and a useful measure of deviation from stoichiometry. Compositions below the Di-CaTs join have more than four cations per six-oxygen formula unit, indicating interstitial cations, anion vacancies or analytical error.

Compositions above the Di-CaEs join contain more silicon than can be accommodated in the tetrahedral sites and must have M-site silicon. The intersection of the Si = 2.5 contour with the Di-CaTs join at negative CaTs content (Fig. 2) corresponds to a composition with no vacancies and 0.5 M-site Si ($CaMg_{1.5}Al_{-1}Si_{2.5}O_6$). Although this composition cannot be physically attained in the CMAS system, it is directly related to the sodium pyroxene (NaPx, $NaMg_{0.5}Si_{0.5}Si_2O_{6'}$) described by Angel *et al.* (1988) by the jadeite exchange vector:

$$CaMg_{1.5}Al_{-1}Si_{2.5}O_6 = NaMg_{0.5}Si_{0.5}Si_2O_6$$
$$- NaAlCa_{-1}Mg_{-1}.$$
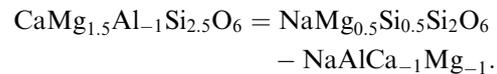
Consequently, stoichiometric sodium pyroxene with octahedral silica can be illustrated in the sodium-free plane by condensing their compositions along the jadeite exchange vector (Thompson, 1982).

The simplicity of the coordinate systems illustrated in Figs 1 and 2 shows that the composition of clinopyroxene can be expressed with equal rigour by using the structural formula or by choosing Qtz (Fig. 1), 3Qtz (Fig. 2a) or CaEs (Fig. 2b) as a component in addition to Di and CaTs. The essential identity of these choices is illustrated in part by the fact that Fig. 2b is entirely contained within Fig. 2a. Because pure CaEs contains 3.5 total cations ($\Sigma = 3.5$), and the mole fractions X_{3Qtz} and X_{Qtz}, in CaEs, are 0.5 and 0.75, respectively, it follows that in clinopyroxene:

$$(4.0 - \Sigma) = X_{3Qtz} = \frac{2X_{Qtz}}{3} = \frac{X_{CaEs}}{2}.$$

One of these coordinate systems may be more convenient or illuminating in a particular circumstance, but they are completely interchangeable, and therefore equivalent. We suggest that using the graphical approach adopted in Fig. 2 simplifies considerations of 'excess silica' and removes ambiguity about its definition.

Excess silica in pyroxene

There are at least five possible definitions of excess silica in stoichiometric and non-stoichiometric pyroxene,

which are conveniently summarized in the model composition space (Fig. 2). Most studies of non-stoichiometric pyroxene have implicitly or explicitly defined excess silica as a deviation from the stoichiometric Di-CaTs join, and have expressed the excess either as a CaEs or Qtz component (e.g. Kushiro, 1969; Bell & Mao, 1971; Wood & Henderson, 1978; Gayk *et al.*, 1995).

Smith & Cheeney (1980) proposed that natural, non-stoichiometric pyroxene has excess silica if $(Si + Ti - 2Na) > (Ca + Mg + Fe + Ni + Mn)$ pfu, and there has been some confusion about the appropriate application of this criterion (Zhang *et al.*, 2002; Klemd, 2003). However, their criterion is directly related to the commonly used definitions of excess silica. The basis of their formulation lies in the algebraic transformation of coordinates from a cation reference frame to calculated end-member formula units (Greenwood, 1975; Spear *et al.*, 1982; Appendix, Table A1). For example, in the four-component system Di-Jd-CaTs-SiO_2, with pyroxene end-members written as six-oxygen formula units, SiO_2 is given by: $SiO_2 = Si-Ca-Mg-2Na$. Consequently, X_{SiO_2} ranges from zero, on the Di-Jd-CaTs plane, to one, at pure SiO_2. If pyroxene contains 'excess' silica, then by definition $SiO_2 > 0$, and $Si-2Na > Ca + Mg$, which is directly analogous to the Smith and Cheeney criterion. Alternatively, if the formula unit for silica is Si_3O_6 (Fig. 2a), $Si_3O_6 = 1/3(Si-Ca-Mg-2Na)$. Either formulation measures the deviation of a composition from the Di-Jd-CaTs plane in terms of excess, pure silica and is, therefore, equivalent to using Qtz as a component. An expanded derivation of the Smith and Cheeney criterion is given in the Appendix.

Stoichiometric pyroxene also may be considered to contain 'excess silica' if $Si > 2$ and M-sites contain silicon. Octahedral coordination of silica is favoured at pressures on the order of 10.0 GPa (Gasparik, 1989). Angel *et al.* (1988) determined the crystal structure of a synthetic sodium pyroxene (NaPx) having the composition $Na(Mg_{0.5}Si_{0.5})Si_2O_6$ and confirmed that the excess silica is accommodated in the octahedral, M1 site. Although sodium pyroxene is supersilicic, because it has $Si > 2$, it does not satisfy the most commonly used definitions of 'excess silica' because it is also stoichiometric and coplanar with Di-Jd-CaTs (Fig. 2).

Khanukhova *et al.* (1976a) suggested a definition of excess silica that can be applied equally well to non-stoichiometric and stoichiometric pyroxene. They considered that 'excess silica' is present if the number of silicon cations pfu is greater than the sum of M-site cations excluding Si (Si:Mcat > 1:1; Fig. 2). Unfortunately, the content of the M-sites remains ambiguous because of the need to make assumptions about the distribution of vacancies between M and T sites, as discussed above. A definition of 'excess silica' that requires silicon to exceed the sum of all other cations (Si:Ocat > 1:1; Fig. 2) would be more robust. End-member NaPx satisfies both definitions of excess silica

because $Si > Mcat$ (2.5Si > 1.5Mcat) or $Si > Ocat$ (2.5Si > 1.5 Ocat).

Both stoichiometric and non-stoichiometric pyroxene may contain 'excess silica'. The various measures of excess silica in non-stoichiometric pyroxene are closely related and internally consistent, but lead to different numerical scales of excess silica content. As shown below, both 'stoichiometric' and 'non-stoichiometric' excess silica can be anticipated in natural and synthetic pyroxene.

Natural and synthetic pyroxene compositions

Figure 3 shows natural and synthetic pyroxene compositions in a portion of Robinson's (1980) 'condensed oxide' space that has the same geometry as Di-CaTs-3Qtz (Fig. 2) and is also similar to a portion of the SAND diagram used by Smith (2006). The choice of end-members and derivation of the plotting coordinates (Fig. 3) are summarized in detail in the Appendix (Table A2). The recalculated analyses are summarized in Tables A3 & A4.

Briefly, the end-member components chosen have 1 Si ($ROR_2O_3SiO_2$), 2 Si ($2RO2SiO_2$) or 3 Si pfu (Si_3O_6), such that each end-member component corresponds to a different independently variable cation. Two end-members with one Si pfu are condensed as the 'Ts' component in Fig. 3 [CaTs (for Al) and $Ca(Mg_{0.5}Ti_{0.5})SiAlO_6$ (for Ti)], whereas the 'Px' component is the sum of nine end-members with 2 Si pfu [diopside (Ca), hedenbergite (Fe^{2+}), enstatite (Mg), johannsenite (Mn), Ni-pyroxene (Ni), kosmochlor (Cr), jadeite (Na), aegirine (Fe^{3+}), and K-pyroxene (K)]. The only end-member containing three Si or vacancies is '3Qtz'. As in Fig. 2, contours of total cations are parallel to the base of the diagram, representing stoichiometric pyroxene, and contours of Si pfu are parallel to the Px-CaEs join. The orientations of other isopleths of cation content are not preserved in the condensed oxide space. Although we have not considered many elements that occur in pyroxene, most common analyses can be plotted in this diagram *directly* from a structural formula or *indirectly* from recalculated end-member components.

End-members were chosen for convenience, subject only to the constraints that: (i) all end-members were calculated with six oxygen and contain at least one silicon; (ii) the end-members be independent and sufficient to span the compositions considered; (iii) only one end-member contains vacancies (3Qtz). Under these conditions, a different choice of end-members, especially for Ti and Fe^{3+}, may change the Ts/Px ratio, but the proportion of 3Qtz remains constant, and does not affect conclusions about excess silica.

The reported compositions of natural omphacite and jadeite are summarized in the Appendix (Table A3) and illustrated in Fig. 3a. Pyroxene compositions that have been 'reconstructed' by reintegration of silica lamellae are not illustrated. The data show excess silica
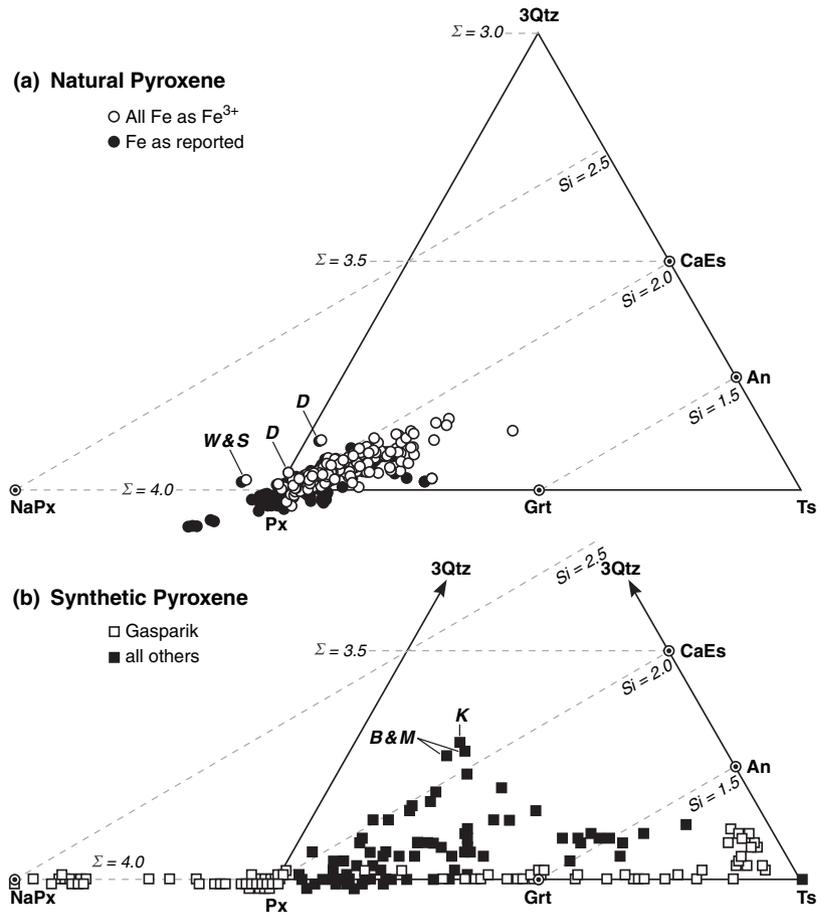
Fig. 3. Natural and synthetic pyroxene compositions in condensed oxide space. (a) Natural pyroxene. Filled circles: analyses with Fe as reported; open circles: all Fe calculated as Fe_2O_3. W&S indicates the sample reported by Wang & Sueno (1996). D indicates two of the samples summarized by Deer *et al.* (1978) (b) Pyroxene compositions synthesized in NCMAS. Open squares: Gasparik (1984a,b, 1985a,b, 1989, 1996). Closed squares: All others (Kushiro, 1969; Bell & Mao, 1971; Khanukhova *et al.*, 1976a,b, 1977; Wood & Henderson, 1978; Wood, 1979). B&M: Bell & Mao, 1971. K: Khanukhova *et al.*, 1976b). Contours of Si and Σ as in Fig. 2. Contours of Ca, Mg and Al are no longer possible because of the projection. Uncertainties ($\pm 2\sigma$) for standard microprobe analyses are probably about one or two times the size of the symbols. The plotting coordinates in terms of cations per six oxygen are: $3Qtz = 0.33(Si + Ti - Fe^{2+} - Mn - Ni - Mg - Ca) - 0.67(Na + K)$; $Ts = Ti + 0.5(Al + Cr + Fe^{3+} - Na - K)$; $Px = -Ti - 0.25(Al + Cr + Fe^{3+}) + 0.5(Fe^{2+} + Mn + Ni + Mg + Ca) + 1.25(Na + K)$ (Table A2).

up to about 11 mol.% 3Qtz (22% CaEs component) and contain up to 27% of Ts components (or more if all iron is calculated as Fe^{3+}). Synthetic pyroxene compositions span the entire stoichiometric pyroxene join from NaPx to Ts (Fig. 3b). Similar to the natural data, the synthetic compositions occupy the region between the Px-Ts and Px-CaEs joins and extend beyond them in both directions. In contrast to the natural data, however, synthetic pyroxene contains up to 28% 3Qtz (56% CaEs; Bell & Mao, 1971) indicating excess silica in the octahedral site up to ~2.1 Si pfu.

The synthetic compositions are iron-free, and the small scatter below the stoichiometric join may give a reasonable indication of uncertainties resulting from analytical error. However, the natural compositions include many analyses in which iron was reported as FeO, as well as some that reported both FeO and Fe_2O_3. The natural pyroxene ranges to −11% 3Qtz and to −13% Ts components. Although negative Ts might correspond to the NaPx component in the pyroxene, and negative 3Qtz corresponds to excess cations, two lines of evidence suggest that the negative values are primarily the result of unanalysed ferric iron. First, most of the pyroxene for which ferric iron was reported contains only positive Ts or 3Qtz (Table A3, Eskola, 1921; Sobolev *et al.*, 1968; Deer *et al.*, 1978;

Bakun-Czubarow, 1992). Second, the calculation of some iron as Fe^{3+} is sufficient to remove most of the negative Ts and 3Qtz components (Fig. 3a). This behaviour is required because calculation of Fe^{3+} has the effect of reducing the number of total cations, thus increasing the amount of 3Qtz. In our calculation scheme, Fe^{3+} is calculated as aegirine and combined with Na in the Px component, thus releasing Al from jadeite to form additional Ts component.

The effects of analytical uncertainty are difficult to evaluate carefully because few authors have presented discussions of uncertainty that are adequate for the task. Microprobe analyses of homogeneous, coarse-grained natural samples may lead to uncertainties in Σ and Si that are quite modest (± 0.007 and ± 0.01, 2σ, respectively). This estimate is based on the propagated uncertainties in the analysis of a standard augite, as described by Giaramita & Day (1990), (Table 2). Wood (1979) reported the standard deviations of multiple analyses for synthetic pyroxene, analysed using an electron microscope microanalyser. The propagated uncertainties of Σ and Si in a typical analysis are larger than conventional microprobe analyses (± 0.07 and ± 0.09, 2σ respectively; sample C164, Table 3; Wood, 1979). Taken together, these results suggest that the small scatter of synthetic compositions

Table 2. Mass balances in CMAS. All reactions were calculated using program REACTION (Finger & Burt, 1972).

REACTION	Di	Prp	Qtz	Ky	mc	tk	vs
			Phase components				
R1	**−1**	**0**	**3**	**0**	**0**	**0**	**−1**
R2 = −R3−2R9	0	1	4	−4	0	3	0
R3	**2**	**−1**	**0**	**0**	**2**	**1**	**0**
R4 = −R1+R9	0	0	−5	2	−1	−2	1
R5 = 4R1+5R3+6R9	0	−5	0	12	4	−7	−4
R6 = −2R1−R3	0	1	−6	0	−2	−1	2
R7 = 3R1+2R3+R9	0	−2	7	2	3	0	−3
R8 = −2R1−3R9	5	0	0	−6	3	6	2
R9	**−1**	**0**	**−2**	**2**	**−1**	**−2**	**0**
R10 = 2R1+6R3+3R9	7	−6	0	6	9	0	−2
R11 = 4R1+3R3+6R9	−4	−3	0	12	0	−9	−4
R12 = −2R3−R9	−3	2	2	−2	−3	0	0
All reactions in the R1–R3 plane conserve Ky							
R6 = −2R1−R3	0	1	−6	0	−2	−1	2
All reactions in the R1–R9 plane conserve Prp							
R4 = −R1+R9	0	0	−5	2	−1	−2	1
R8 = −2R1−3R9	5	0	0	−6	3	6	2
All reactions in the R3–R9 plane conserve vs							
R2 = −R3−2R9	0	1	4	−4	0	3	0
R12 = −2R3−R9	−3	2	2	−2	−3	0	0
All reactions in the R3–R8 plane conserve Qtz							
R5 = 5R3−2R8	0	−5	0	12	4	−7	−4
R10 = 6R3−R8	7	−6	0	6	9	0	−2
R11 = 3R3−2R8	−4	−3	0	12	0	−9	−4
All reactions in the R2–R4 plane conserve Di							
R5 = −5R2−4R4	0	−5	0	12	4	−7	−4
R6 = R2+2R4	0	1	−6	0	−2	−1	2
R7 = −2R2−3R4	0	−2	7	2	3	0	−3

Table 3. Qtz-forming reactions in CMAST. Labels in parentheses indicate reactions in Tables 2 and A6.

Reactions that conserve both *vs* and *ts* components
4Ky	= 4Qtz + Prp + 3tk	(R2)
2Ky	= 2Qtz + Di + mc + 2tk	(−R9)
3Di + 2Ky + 3mc	= 2Qtz + 2Prp	(R12)
Di + 2Rt + mc	= 2Qtz + 2Gk	(GR4)
Ky + Rt	= 2Qtz + Gk + tk	(−GR6)
Prp + Rt	= 4Qtz + 4Gk + tk	(−GR9)
Prp + 3Rt	= 2Qtz + Ky + 3Gk	(−GR10)

Reactions that conserve *vs* component and control *ts* content
Rt	= Qtz + ts	(Rt1)
Ky + ts	= Qtz + Gk + tk	(G3)
Ky + 3Gk	= Qtz + Prp + 3ts	(G4)

Reactions that control *vs* content
Di + vs	= 3Qtz	(R1)
2Ky + vs	= 5Qtz + mc + 2tk	(R4)
Prp + 2vs	= 6Qtz + 2mc + tk	(R6)
2Prp + 3vs	= 7Qtz + 2Ky + 3mc	(R7)
2Gk + vs	= Qtz + 2Rt + mc	(GR2)
Gk + vs	= 3Qtz + mc + 2ts	(−G5)

below the Px-Ts join and above the Px-Es join reflects analytical uncertainties. However, some sodic and calcic pyroxene compositions probably represent stoichiometric and non-stoichiometric phases with Si > 2 (Fig. 3b, Bell & Mao, 1971; Khanukhova *et al.*, 1976b; Gasparik, 1989).

Natural pyroxene shows little evidence for excess silica in the octahedral site (Si > 2), outside the uncertainty because of analytical error or unanalysed ferric iron. Only two jadeite analyses (D, Fig. 3a; Deer *et al.*, 1978, table 49, nos 6 & 9; Table A3) contain Si significantly greater than two, and should be viewed skeptically. However, Wang & Sueno (1996) reported an inclusion in diamond with a composition approximately $NaPx_{16}En_{84}$, which requires Si > 2 (W&S, Fig. 3a). On the basis of experimental results (Gasparik, 1989), they predicted that this pyroxene composition should have a garnet structure. Wang & Gasparik (2000) described unpublished data that show that the inclusion does indeed have the garnet structure and must have been derived from pressures greater than 16.5 GPa. The recognition of such garnet inclusions suggests that appropriate compositions exist in the mantle to stabilize NaPx as a component in pyroxene at slightly lower pressures, below the pyroxene–garnet transition. Thus, it should be anticipated that stoichiometric, supersilicic pyroxene might be recovered from the mantle.

The data demonstrate that two distinct kinds of 'excess' silica may be anticipated in both nature and experiments. Stoichiometric pyroxene may be considered to contain 'excess' silica if Si > 2 whereas non-stoichiometric pyroxene containing vacancies may have Si < 2, but requires compositions that lie on the silica-rich side of the stoichiometric pyroxene join (Figs 1–3). In the following section, we explore the mechanisms by which free silica may be formed in eclogite and whether these two kinds of excess Si lead to different mechanisms. The approach begins by examining the set of all possible reactions in model eclogite compositions using a Thompson reaction space (Thompson, 1982). It is shown that free silica can be formed not only by the consumption of vacancies in non-stoichiometric pyroxene, but also by reaction with accessory phases and by dissolving ilmenite or rutile in pyroxene or garnet.

A REACTION SPACE FOR ECLOGITE

The analysis of all possible reactions is begun by constructing a reaction space based on common phases in the system CaO-MgO-Al_2O_3-SiO_2 (CMAS). The major phases in eclogite are clinopyroxene (Cpx) and garnet (Grt). Common accessory phases in a model eclogite might include a silica polymorph, summarized as quartz, and an aluminium silicate polymorph, assumed to be kyanite. For the purpose of balancing reactions, SiO_2 is used, rather than Si_3O_6, as the formula unit for Qtz because reaction coefficients are simpler. We then examine the effects of additional components and phases, and expand the reaction space to include Ti-bearing accessory minerals.

Derivation in CMAS

A model eclogite in CMAS (Fig. 1) requires four independent system components. If four or fewer phases are present (e.g. clinopyroxene, garnet, kyanite, and quartz or coesite), and polymorphic transitions are ignored, most reactions are continuous and have two or more degrees of freedom in the phase rule. In order

to describe the continuous reactions, it is useful to choose independently variable phase components sufficient to describe the possible variations of the modes and compositions of the phases (Thompson, 1982). Typically, one chooses a single end-member as the additive component for each phase, which monitors the abundance of the phase, and a number of exchange components, which describe variations of phase composition but have no effect on phase abundances (Thompson, 1982). Table 1 lists the formula units of end-members, additive components and exchange components that will be considered here. Because it is important to distinguish between mineral phases and phase components, abbreviations are used for phase components and full names for mineral phases.

The possible modal and compositional variations of eclogite phases in CMAS can be described with seven independently variable phase components (Di, Prp, Ky, Qtz, *mc, tk, vs*, Table 1). It was assumed that silica and aluminium silicate polymorphs have constant compositions and need only additive components, Qtz and Ky, but both clinopyroxene and garnet display extensive solid solution (Fig. 1). The Di end-member was chosen as the additive component for clinopyroxene, but *any* end-member pyroxene could have been used. All variations of stoichiometric clinopyroxene towards end-member enstatite, wollastonite, or calcium Tschermak pyroxene can be described by linear combinations of the additive component, Di, and two exchange components, *tk* and *mc* (Table 1). All non-stoichiometric clinopyroxene compositions above the En-Wo-CaTs-MgTs join (Fig. 1) can be described using the additional vacancy-silicon exchange component, *vs* (e.g. CaEs = Di + 0.5*tk* + 0.5*vs*). The Prp end-member was chosen as the additive component for garnet, and variations of composition towards grossular and majorite garnet may be described using the *mc* and *tk* exchanges. For this study, it was assumed that *vs* component is *nil* in garnet (but see W&S; Fig. 3a and Smith, 2006). These seven additive and exchange components are sufficient to monitor progress on all possible net-transfer and exchange reactions in model eclogites in CMAS.

Inspection of Fig. 1 shows that no more than four independent components are required in order to describe the four phases clinopyroxene, garnet, kyanite and quartz. Singular value decomposition of the composition matrix (Fisher, 1989; Appendix, Table A5) confirms that four independent system components are necessary and sufficient to describe the seven phase components, and that three independent mass balances (or reactions) are necessary and sufficient to describe all mass balances among the phase components.

Although the results of singular value decomposition provide one possible choice of three independent reactions (Table A5), it proved more convenient to choose three reactions from the set of all possible balanced reactions among phase components calculated using the program REACTION (Table 2) (Finger &

Burt, 1972; see Andrew & Linde, 1980, for a cautionary note). Three useful mass balances, R1, R3, and R9, were chosen as basis vectors of a reaction space (Fig. 4a):

$$Di + vs = 3Qtz \qquad (R1)$$

$$Prp = 2Di + 2mc + tk \qquad (R3)$$

$$Di + 2Qtz + mc + 2tk = 2Ky. \qquad (R9)$$
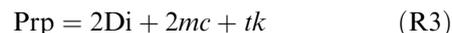
Simple inspection shows that the three mass balances are independent because each contains a unique phase component. The exchange component *vs* appears only in R1, and the additive components Prp and Ky appear only in R3 and R9, respectively. The three mass balances also are sufficient to span the reaction space because all other mass balances can be formed as linear combinations of the three basis vectors, as shown in Table 2.

The exchange components have not been assigned to phases, and it is not necessary to do so in order to evaluate all possible net-transfer reactions. Although *vs* is best known in pyroxene, the *tk* and *mc* exchanges are important in both pyroxene and garnet (e.g. Thompson, 1982). Identification of the exchange capacities with particular phases greatly increases the number of possible reactions, but does not change the essential nature of the net transfers involved. For example, if the generalized *tk* and *mc* components are identified with garnet and clinopyroxene (tk_{Grt}, tk_{Cpx}, mc_{Grt}, mc_{Cpx}), the number of calculated net-transfer reactions expands from 12 (Table 2) to 35. The new net transfers are all related to one or more companion reactions by two exchange reactions ($tk_{Grt} = tk_{Cpx}$, $mc_{Grt} = mc_{Cpx}$). The exchange reactions control the phase in which the exchange capacity is located (i.e. the composition of the phases), but have no effect on the abundance of phases participating in the net transfers. Consequently, no new information about the nature of the net-transfer reactions is gained by assigning exchange capacity to specific phases.

Properties of the CMAS reaction space

The three basis vectors define a three-dimensional reaction space (Fig. 4a) and monitor different aspects of eclogite mineralogy. Positive progress on the basis vectors is defined as progress to the right as written above, and is illustrated by the arrows (Fig. 4a). Reaction R1 is the only basis vector that contains the exchange component *vs*, so it is a useful monitor of the vacancy content of clinopyroxene. Reaction R3 involves only the major phases garnet and clinopyroxene. It is the only reaction that involves no accessory phase, such as quartz or kyanite (Table 2). Because *mc* and *tk* exchange capacity are found only in clinopyroxene and garnet, R3 monitors the pyroxene to garnet transition and the changing compositions of
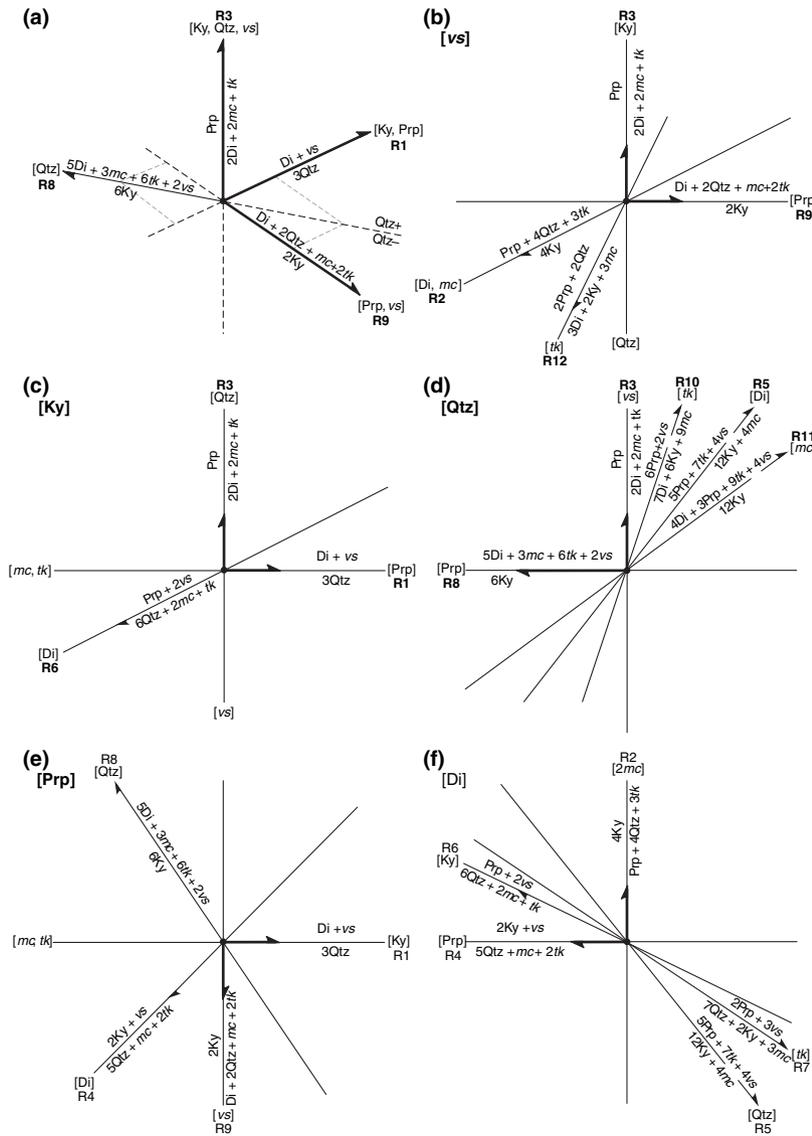
Fig. 4. Reaction space for eclogite in CMAS. All reactions among phase components are positive as written in Table 2. Basis vectors are shown as heavy arrows with arbitrary unit lengths and are positive in the direction shown by arrows. Reactants written on same side of reaction as arrowhead. Components written in square brackets are conserved in the labelled reaction. The component written in the top left of each figure is conserved in all reactions in that plane. (a) Basis vectors in the three-dimensional reaction space. Reaction R8 is a Qtz-conservative reaction that lies in the R1–R9 plane. Reactions R8 and R3 define a Qtz-conservative plane that separates Qtz-producing and Qtz-consuming half-spaces. All linear combinations of the basis vectors that pass behind this plane produce Qtz; those that pass in front consume Qtz. All subsequent diagrams illustrate a plane in the reaction space. (b) R3–R9 plane. Contains all [vs] reactions. (c) R3–R1 plane. Contains all [Ky] reactions. (d) R3–R8 plane. Contains all [Qtz] reactions. (e) R1–R9 plane. Contains all [Prp] reactions. (f) R2–R4 plane. Contains all [Di] reactions.

the two phases during the transition. Reaction R9 involves the accessory phases quartz and kyanite and is the only basis vector involving Ky.

The three-dimensional reaction space (Fig. 4a) includes all possible net-transfer reactions in the model eclogites, which must be linear combinations of the three basis vectors. All reactions lie in one of five key planes in the reaction space (Fig. 4b,f), which are a convenient summary of the kinds of net-transfer reactions that are possible in CMAS. The reactions that conserve *vs* component lie in the R3–R9 plane (Fig. 4b) and are useful for considering stoichiometric pyroxene. Any direction in reaction space that does not lie in the R3–R9 plane represents a reaction that consumes or produces vacancies in pyroxene.

Two planes are particularly useful for examining eclogites that lack kyanite or quartz as accessory minerals. The R3–R1 plane (Fig. 4c) contains reactions that conserve the additive component (and phase) Ky. The R3–R8 plane (Fig. 4d) includes the reactions that conserve the additive component (and phase) Qtz. Any reaction vector not in this plane produces or consumes free silica.

The R1–R9 plane (Fig. 4e), which contains all reactions that conserve additive Prp, illustrates two independent ways in which free silica can be produced. The consumption of vacancies in non-stoichiometric pyroxene yields free silica as does the decomposition of kyanite to a stoichiometric pyroxene and a silica polymorph. Note that the latter reaction could also proceed with non-stoichiometric pyroxene as long as *vs* is conserved.

The plane R2–R4 (Fig. 4f) contains all Di-conservative reactions, including R7. This plane is not easily visualized in Fig. 4a because it is defined by R2 (in the R3–R9 plane, Fig. 4b) and R4 (in the R1–R9 plane;

Fig. 4e). All diopside-conservative reactions involve one or more of the two accessory phases, kyanite and quartz (Table 2).

Other components and phases

Although jadeite is a major constituent of omphacite, sodium was not included in the model reaction space because it does not require the presence of a new eclogite phase. Consequently, the number and nature of the net-transfer reactions remain unchanged. Likewise, the net-transfer reactions are not affected by the presence of a second pyroxene, such as enstatite. Because diopside and enstatite compositions are simply related ($Di + mc = En$), the additive component Di may be used to represent total pyroxene without serious inconvenience. Although phase rule variance changes if a second pyroxene is present, the basic nature of the net transfer does not, so a second pyroxene phase was not included in the model.

It is useful to consider the effects of titanium on the model reactions because ilmenite and rutile are common accessory phases in eclogite (e.g. Smith, 1988), and reactions of any non-silicate phase with silicate minerals may release free silica. All variations of Ti content in pyroxene and garnet can be expressed with a single additional exchange component: $ts = TiSi_{-1}$. It is important to note that the ts exchange does not necessarily imply tetrahedral coordination of titanium because ^{VI}Ti might be incorporated through the exchange $^{VI}Ti^{IV}Al$ ($^{VI}Al^{IV}Si)_{-1}$, which is equivalent to ts (Müntener & Hermann, 1994; Labotka, 1995). Papike (1980) noted that Al and Ti contents of pyroxene are highly correlated and suggested that the substitution takes place by a Ti-Tschermak type of exchange ($TiAl_2Mg_{-1}Si_{-2}$), which is equivalent to $ts + tk$. Labotka (1995) concluded that Ti variability in garnet is best described by using the component $Ca_3Mg_{0.5}AlTi_{1.5}Si_2O_{12}$, which corresponds to $Grs + 1.5ts - 0.5tk$. Note, however, that the addition of ts component has no effect on the number or kind of net-transfer reactions present, unless an additional phase is stabilized.

The effects of ilmenite and rutile on the production or consumption of free quartz can be modelled in CMAST if geikielite ($MgTiO_3$) is used as a proxy for ilmenite. All reactions involving rutile or geikielite in the expanded model system can be described with the addition of two new basis vectors (Appendix; Table A6):

$$Rt = Qtz + ts \qquad (Rt1)$$

and

$$Di + mc + 2ts = 2Gk. \qquad (G1)$$

Table 3 summarizes all 16 reactions that involve quartz in the expanded model system. In the absence of geikielite, the basis vector for rutile Rt1 is the only new reaction in CMAST that releases free silica. The basis vector for geikielite G1 involves no free silica and is not shown in Table 3. It describes the precipitation of geikielite from pyroxene by consumption of En ($Di + mc$) and ts components. In the absence of rutile, Gk participates in only three reactions involving Qtz (G3, G4 & G5; Table 3), each of which conserves Di. The basis vector Rt1 may be used to eliminate ts component from previously derived Rt-conservative reactions (G1, G2, G3 G5 & R12; Tables 2, 3 & A6) leading to five new reactions among Gk, Rt and Qtz (GR reactions, Table 3). Such reactions illustrate how silica may be released in the presence of rutile and ilmenite (Gk) *without* changing the titanium (ts) content of any phase.

DISCUSSION

'Excess silica' and pyroxene compositions

'Excess silica' may be present in both stoichiometric and non-stoichiometric pyroxene. In non-stoichiometric pyroxene, 'excess' is commonly defined as the amount of silica beyond that needed to form stoichiometric pyroxene. Such pyroxene is not rare in eclogite and are easily identified by having a deficiency of cations ($\Sigma < 4$) outside analytical uncertainty. Stoichiometric pyroxene may also be considered to contain 'excess' silica if Si < 2. Both sodium and calcium pyroxene with Si > 2 have been synthesized, and the octahedral coordination of Si has been confirmed (Bell & Mao, 1971; Angel *et al.*, 1988; Gasparik, 1989). Although stoichiometric pyroxene with Si > 2 has yet to be demonstrated in nature, a garnet inclusion in diamond has the composition of a supersilicic pyroxene with both kinds of excess silica, because it has Si > 2 and $\Sigma < 4$ (Fig. 3a; Wang & Sueno, 1996). This garnet, therefore, contains excess silica (cf. Smith, 2006) and suggests that similar pyroxene might be recovered from the mantle.

For the purpose of precise scientific communications, it is useful to have a common means of describing pyroxene composition and 'excess silica'. The mole fraction of 3Qtz (or 'supersilipyx', Smith, 2006) is a convenient component to express 'excess silica' in non-stoichiometric pyroxene because it is pure silica, it is numerically equivalent to the cation deficiency in a six-oxygen formula unit, and isopleths of constant Si content are parallel and evenly spaced in simple composition diagrams (Figs 2 & 3). Nevertheless, Qtz or CaEs are acceptable and directly related to the cation deficiency [$(4.0 - \Sigma) = X_{3Qtz} = 2X_{Qtz}/3 = X_{CaEs}/2$]. If excess silica is the primary focus of a study, it is convenient that the values of these mole fractions are not affected by the choice of other pyroxene components, as long as those components are based on six oxygen formula units and only one component is chosen to contain vacancies. The cationic criterion for excess silica (Smith & Cheeney, 1980) is equivalent to using SiO_2 as a component. Because all

such criteria are internally consistent and directly related, they are considered to be equivalent and interchangeable.

We have shown that the term 'excess' silica has been used in at least five ways, most commonly for a composition that contains more silica than a stoichiometric pyroxene with no vacancies, but also for pyroxene containing more than 2 Si pfu. The term 'supersilicic' is also commonly used in the literature and Smith (2006) has suggested that the term should be synonymous with 'excess silica' and restricted to non-stoichiometric compositions having the ability to exsolve SiO_2 and leave behind a stoichiometric pyroxene. His approach leaves no way to describe stoichiometric pyroxene with Si > 2, which we would describe as 'supersilicic'. We have also been hesitant to accept this definition because the ability to exsolve SiO_2 depends upon the location of the silica saturation surface in composition space (e.g. Khanukhova *et al.*, 1976a,b, 1977), which may vary with *P*–*T*, or mineral assemblage. Thus, a sample of given 3Qtz content would contain 'excess silica' at conditions of super-saturation but would not contain 'excess silica' at conditions where the same composition is under-saturated.

One way of resolving the terminology dilemma might be to use 'excess silica', 'supersilicic' and 'silicic' to describe compositions without reference to silica saturation. 'Excess silica' could be a general term requiring definition in context. 'Supersilicic' could be used to describe any pyroxene with Si > 2 and 'silicic' might refer to all pyroxene compositions that have Si < 2, but greater than the variable Si in stoichiometric pyroxene. Alternatively, it may be simpler and less contentious to define the terms as necessary for clarity.

We have depended heavily on standard algebraic methods (e.g. Greenwood, 1975; Spear *et al.*, 1982) to calculate pyroxene compositions and to derive plotting coordinates for simple composition diagrams (see Appendix). Page *et al.* (2005) suggested that the 'matrix method' systematically overestimates 'excess silica' in pyroxene and pointed to several discrepancies in the literature. Any mineral composition may be described completely and rigorously using a wide variety of possible components: cations pfu, end-members, or additive and exchange operators. If the transformation from one coordinate system to another is done rigorously, by matrix inversion or otherwise, the coordinate systems are interchangeable and, to that extent, equivalent. One coordinate system might be more effective than another for calculation, pedagogy, or illustration, but the method of calculating the components should not affect any conclusion derived from the data. Typically, we reproduced precisely the results of well-known data sets in the literature by several methods of calculation. Discrepancies cited by Page *et al.* (2005) between estimates of excess silica based on structural formulas and those based on algebraic calculations of end-member components probably are artifacts of unstated assumptions, approximations, or errors by earlier authors. With an appropriate choice of components, all methods of calculating 'excess silica' are equivalent.

Formation of free silica

Stoichiometric pyroxene

If pyroxene and garnet are stoichiometric and contain no *vs* components, all reactions must conserve *vs* component, and free silica can form only by reactions with accessory phases (Table 3). This is clearly demonstrated in the CMAS system, in which all reactions that conserve the *vs* component of pyroxene lie in the R3–R9 plane (Fig. 4b). These are the only reactions that can be used to describe processes involving stoichiometric, vacancy-free pyroxene. In the absence of accessory phases, R3 is the only possible reaction. This reaction monitors the pyroxene to garnet transition and associated changes of mineral composition. All other reactions involving stoichiometric pyroxene in CMAS (R2, R9 & R12; Table 3) must involve both kyanite and quartz, and a change in the abundance of one accessory mineral requires a complementary change in the other. Note that all reactions in the R3–R9 plane can also proceed with non-stoichiometric pyroxene, as long as the *vs* component is conserved.

All net-transfer reactions that require titanium as an additional component necessarily involve an accessory phase such as rutile or geikielite, our proxy for ilmenite (Appendix Table A6). Seven reactions conserve the *vs* component and can be used to describe silica precipitation involving stoichiometric pyroxene (Table 3). Four of the seven reactions (GR4, GR6, GR9 & GR10; Table 3) produce geikielite and quartz by reaction of rutile with other phases and do not require a change in the titanium content of any phase. In particular, reaction GR4 suggests that rutile inclusions in pyroxene might react with En component (Di + mc) to produce geikielite (or ilmenite) and free quartz. Three other reactions involve the *ts* component (Rt1, G3 & G4; Table 3). The basis vector for rutile (Rt1, Table 3) implies that consuming (or dissolving) rutile as *ts* component in either garnet or pyroxene releases free silica.

Non-stoichiometric pyroxene

In the absence of accessory phases, all reactions capable of producing free silica proceed by the consumption of the vacancies in non-stoichiometric pyroxene (Table 3). In CMAS, reactions that conserve accessory Ky occur in the R3–R1 plane (R1, R6; Table 2; Fig. 4c). Reaction R3 neither produces nor consumes Qtz. Reaction R1 produces Qtz at the expense of the Di and *vs* components of pyroxene, whereas R6 yields Qtz at the expense of Prp and *vs* components. In the absence of accessory Ky, therefore, all mechanisms of

producing the free silica in CMAS eclogites require the destruction of vacancies in non-stoichiometric pyroxene.

The destruction of vacancies does not necessarily require the precipitation of free silica, however. This is demonstrated in Fig. 4d, which illustrates the reactions that conserve Qtz in the R3–R8 plane. Most of these reactions consume vacancies while producing Ky (R5, R8, R10 & R11; Table 2), and may help control the compositions of pyroxene and garnet in kyanite eclogite. Reaction R8 may provide a mechanism for the precipitation of aluminium silicate inclusions in pyroxene (Williams, 1932; O'Hara & Yoder, 1967).

All other reactions involving accessory kyanite and *vs* component that also release free silica are contained in the Di-conservative plane (Fig. 4f). Four of the five reactions in Fig. 4f (R2, R4, R6 & R7; Table 2) release Qtz at the expense of Prp or Ky. Note that the production of free silica by these reactions does not require the consumption of additive pyroxene, although the composition of the pyroxene may change because of the exchange components participating in the reactions.

If titanium is added to the model system, only two additional net-transfer reactions describe interactions between accessory phases and non-stoichiometric pyroxene. Reaction G5 (Table 3) provides a mechanism by which geikielite (or ilmenite) inclusions could react with vacancies in host pyroxene to produce free silica. Reaction GR2 (Table 3) consumes vacancies to produce free silica and rutile, but does not require a change in the titanium content (*ts*) of any phase.

Controls on silica precipitation in eclogite

The reactions in CMAST demonstrate three broad controls on the precipitation of free silica in eclogite: (i) the presence or absence of accessory phases; (ii) the titanium content of pyroxene or garnet; (iii) the vacancy content of pyroxene.

Table 3 demonstrates the critical role of accessory phases in the formation of free silica. All but two of the 16 reactions (R1 & R6) require the presence of an accessory phase (kyanite, rutile or geikielite). Eclogite with stoichiometric pyroxene may form free silica *only* by the first 10 reactions, all of which require an accessory phase as a reactant and conserve *vs* component. In the absence of accessory phases, free quartz cannot form by reaction in an eclogite with stoichiometric pyroxene. This restriction also applies to supersilicic (Si > 2), stoichiometric pyroxene with elevated NaPx content, because their compositions are coplanar with the more familiar stoichiometric pyroxenes (Figs 2 & 3). Obviously, this conclusion does not mean that eclogite could not already be saturated with excess silica because of bulk chemical composition.

The titanium content of pyroxene and garnet might also be an important control on the formation of free silica. The precipitation of free silica will accompany the dissolution of rutile as *ts* component in either pyroxene or garnet (Rt1, Table 3) or the dissolution of ilmenite in pyroxene at the expense of the *vs* component (G5, Table 3). Consequently, any change in physical conditions that affects rutile or ilmenite saturation in eclogite, will also affect the balance of free silica. Reactions G3 and G4, also demonstrate that titanium saturation in the stability field of quartz + kyanite + geikielite (or ilmenite) may affect the precipitation of free silica.

Silica precipitation is also controlled by the vacancy (*vs*) content of non-stoichiometric pyroxene through six reactions. Reaction R1 (Table 3) corresponds to the direct precipitation of free silica from clinopyroxene, but all the other reactions require the interaction of another phase with the vacancies in clinopyroxene. These reactions suggest that inclusions of garnet, kyanite or ilmenite (Gk) could interact with vacancies in the host pyroxene to produce free silica. It is possible that the balance of free silica might be affected as much by these interactions as by the direct precipitation of silica via reaction R1 (Table 3).

It is important to note that vacancy content cannot be an independent monitor of the potential to produce free silica, because vacancies can be consumed without the precipitation of free silica (Fig. 4d). Moreover, silica can be released by mechanisms that do not involve vacancies.

Titanium and vacancy contents might be equally important controls on the balance of free silica in eclogite. Pyroxene is known to contain as much as 0.3 Ti (Robinson, 1980, Table 1) and cation deficiency as high as 0.3 ($\Sigma = 3.7$, Fig. 3; Bell & Mao, 1971), but the effects of *P–T* and phase assemblage on Ti and vacancy contents are poorly understood.

There seems little doubt that high pressures favour the stability of non-stoichiometric pyroxene (Khanukhova *et al.*, 1976a,b, 1977; Wood & Henderson, 1978; Wood, 1979; Gasparik & Lindsley, 1980; Gasparik, 1984a). Although it seems reasonable to infer that free silica might be released on decompression, considerable caution is warranted because the effects of pressure vary with mineral assemblage in both true eclogite and plagioclase-bearing assemblages and have not been explored systematically. The vacancy content of clinopyroxene coexisting with plagioclase or plagioclase + quartz, in the CMAS and NCAS systems, increases with pressure up to about 3.0 GPa (Wood, 1979; Gasparik & Lindsley, 1980; Gasparik, 1985a). At higher pressures, however, vacancy content shows a strong negative dependence on pressure in the assemblage Cpx + Pl + Qtz, and little or no variation with *P–T* in the 'eclogite' assemblage Cpx + Grs + Ky + Qtz (Gasparik, 1985a). Sekine *et al.* (1986) and Irifune *et al.* (1986) also found that the CaEs content of pyroxene is approximately constant in eclogite of MORB composition in the pressure region 5.0–9.5 GPa, above which the CaEs content decreases

markedly, as stishovite is precipitated. Okamoto & Maruyama (2004) reported a similar decrease of CaEs content at somewhat lower temperatures in the region 10.0–18.0 GPa.

The available evidence shows that high pressure favours low titanium content of clinopyroxene. Yagi & Onuma (1967) successfully synthesized aluminous diopside containing up to about 0.2 Ti pfu at atmospheric pressure, whereas, at 1.0–2.5 GPa, the solubility of Ti was *nil*. These results are reinforced by data showing that Ti substitutions in pyroxene increase the molar volume (Onuma *et al.*, 1968; Redhammer *et al.*, 2003). Zhang *et al.* (2003) conducted experiments on a natural ilmenite-rich garnet clinopyroxenite at pressures from 4 to 10 GPa. They found that diopside-rich clinopyroxene contained only about 0.01 Ti pfu, despite saturation with ilmenite or rutile, and that Ti content was only a weak function of pressure. On the other hand, coexisting garnet contained up to 0.25 Ti pfu and Ti content was strongly dependent on pressure. Both lines of evidence suggest that Ti saturation decreases in clinopyroxene with increasing pressure.

As lower pressures appear to favour higher Ti and lower vacancy contents in clinopyroxene, reactions R1 and Rt1 should each proceed in the direction that precipitates free silica during decompression from the coesite stability field (Table 3). Thus, both solution of rutile and destruction of vacancies may contribute to growth of quartz or coesite lamellae in clinopyroxene. At pressures above 9.5 GPa, in the stishovite field, free silica may be released as pressure increases (Sekine *et al.*, 1986).

We have not attempted an exhaustive exploration of pyroxene composition space or of the implications of other possible accessory phases for the origin of free silica in eclogite (e.g. titanite, phosphate, carbonate). Nevertheless, our observations suggest that, in the most common eclogite compositions, reliable interpretation of the significance of silica lamellae and inclusions in natural clinopyroxene will require the evaluation not only of silica solubility, but also Ti solubility, and the possible roles of accessory phases and inclusions on the balance of free silica.

CONCLUSIONS

'Excess silica' may be found in either stoichiometric or non-stoichiometric pyroxene, but the meaning of 'excess' is different in the two cases. In the first instance, Si cations exceed the amount that can be accommodated in the tetrahedral site of a pyroxene. In the second, the composition of a pyroxene with vacancies in the M-sites can be described as a stoichiometric pyroxene plus excess silica. Nevertheless, we find that all commonly used reference frames or definitions of excess silica in non-stoichiometric pyroxene are internally consistent, interchangeable, and therefore equivalent.

Our examination of all possible net-transfer reactions in simple model eclogite shows that there are three broad mechanisms by which free silica can be released: (i) vacancy consumption in non-stoichiometric pyroxene; (ii) dissolution of rutile or ilmenite in pyroxene or garnet; (iii) reactions among accessory phases, garnet and pyroxene.

The vacancy content of pyroxene cannot be used as an independent monitor of the potential for producing free silica because vacancies can be consumed by Qtz-conserving reactions and silica can be released by reactions not involving vacancies.

REFERENCES

Andrew, A. S. & Linde, J., 1980. MRF: A FORTRAN IV computer program for the generation of univariant phase equilibria. *Computers & Geosciences*, **6**, 227–236.

Angel, R. J., Gasparik, T., Ross, N. L., Finger, L. W., Prewitt, C. T. & Hazen, R. M., 1988. A silica-rich sodium pyroxene phase with six-coordinated silicon. *Nature*, **335**, 156–158.

Bakun-Czubarow, N., 1992. Quartz pseudomorphs after coesite and quartz exsolutions in eclogitic omphacites of the Złote Mountains in the Sudetes (SW Poland). *Archiwum Mineralogiczne*, **48**, 3–25.

Bell, P. M. & Mao, H. K., 1971. Composition of clinopyroxene in the system $NaAlSi_2O_6$–$CaAl_2Si_2O_8$. *Carnegie Institution of Washington Yearbook*, **70**, 131.

Clark, S. P., Schairer, J. F. & de Neufville, J., 1962. Phase relations in the system $CaMgSi_2O_6$–$CaAl_2SiO_6$-SiO_2 at low and high pressure. *Carnegie Institution of Washington Yearbook*, **61**, 59–68.

Deer, W. A., Howie, R. A. & Zussman, J., 1978. *Rock-forming Minerals, Vol. 2A, Single-chain Silicates*. 668 pp. Wiley, New York.

Dobrzhinetskaya, L. F., Schweinehage, R., Massonne, H. J. & Green, H. W., 2002. Silica precipitates in omphacite from eclogite at Alpe Arami, Switzerland: evidence of deep subduction. *Journal of Metamorphic Geology*, **20**, 481–492.

Doelter, C., 1883. Uber einige Augite von bermerkenswerther Zusammensetzung. *Mineralogische und Petrographische Mittheilungen*, **5**, 224–233.

Eskola, P., 1921. On the eclogites of Norway. Videnskapsselskapets i Kristiana Skrifter I. *Matamatisk - Naturvidenskabelig Klasse*, **8**, 1–118.

Finger, L. W. & Burt, D. M., 1972. Reaction, a FORTRAN IV computer program to balance chemical reactions. *Carnegie Institution of Washington Yearbook*, **71**, 616–620.

Fisher, G. W., 1989. Matrix analysis of metamorphic mineral assemblages and reactions. *Contributions to Mineralogy and Petrology*, **102**, 69–77.

Gasparik, T., 1984a. Experimental study of subsolidus phase-relations and mixing properties of pyroxene in the system CaO-Al_2O_3-SiO_2. *Geochimica et Cosmochimica Acta*, **48**, 2537–2545.

Gasparik, T., 1984b. Experimentally determined stability of clinopyroxene + garnet + corundum in the system CaO-MgO-Al_2O_3-SiO_2. *American Mineralogist*, **69**, 1025–1035.

Gasparik, T., 1985a. Experimental study of subsolidus phase-relations and mixing properties of pyroxene and plagioclase in the system Na$_2$O-CaO-Al$_2$O$_3$-SiO$_2$. *Contributions to Mineralogy and Petrology*, **89**, 346–357.

Gasparik, T., 1985b. Experimentally determined compositions of diopside-jadeite pyroxene in equilibrium with albite and quartz at 1200–1350 degrees-C and 15–34 kbar. *Geochimica et Cosmochimica Acta*, **49**, 865–870.

Gasparik, T., 1989. Transformation of enstatite – diopside – jadeite pyroxenes to garnet. *Contributions to Mineralogy and Petrology*, **102**, 389–405.

Gasparik, T., 1996. Diopside-jadeite join at 16–22 GPa. *Physics and Chemistry of Minerals*, **23**, 476–486.

Gasparik, T. & Lindsley, D. H., 1980. Phase equilibria at high pressure of pyroxenes containing monovalent and trivalent ions. In: *Pyroxenes, Reviews in Mineralogy 7*, (ed. Prewitt, C. T.), pp. 309–340, Mineralogical Society of America, Washington, DC.

Gayk, T., Kleinschrodt, R., Langosch, A. & Seidel, E., 1995. Quartz exsolution in clinopyroxene of high-pressure granulite from the Münchberg massif. *European Journal of Mineralogy*, **7**, 1217–1220.

Giaramita, M. J. & Day, H. W., 1990. Error propagation in calculations of structural formulas. *American Mineralogist*, **75**, 170–182.

Greenwood, H. J., 1975. Thermodynamically valid projections of extensive phase relationships. *American Mineralogist*, **60**, 1–8.

Hays, J. F., 1966. Stability and properties of the synthetic pyroxene CaAl$_2$SiO$_6$. *American Mineralogist*, **51**, 1524–1529.

Hays, J. F., 1967. Lime-alumina-silica. *Carnegie Institution of Washington Yearbook*, **65**, 234–239.

Irifune, T., Sekine, T., Ringwood, A. E. & Hibberson, W. O., 1986. The eclogite-garnetite transformation at high-pressure and some geophysical implications. *Earth and Planetary Science Letters*, **77**, 245–256.

Katayama, I., Parkinson, C. D., Okamoto, K., Nakajima, Y. & Maruyama, S., 2000. Supersilicic clinopyroxene and silica exsolution in UHPM eclogite and pelitic gneiss from the Kokchetav massif, Kazakhstan. *American Mineralogist*, **85**, 1368–1374.

Khanukhova, L. T., Zharikov, V. A., Ishbuatov, R. A. & Litvin, Y. A., 1976a. Excess silica in solid solutions of high-pressure clinopyroxenes as shown by experimental study of the system CaMgSi$_2$O$_6$–CaAl$_2$SiO$_6$ at 35 kilobars and 1200 °C. *Doklady Akademii Nauk SSSR, Earth Sciences Section*, **229**, 170–172.

Khanukhova, L. T., Zharikov, V. A., Ishbulatov, R. A. & Litvin, Y. A., 1976b. Pyroxene solid solutions in the system NaAlSi$_2$O$_6$-CaAl$_2$SiO$_6$-SiO$_2$ system at 35 kbar and 1200 °C. *Doklady Akademii Nauk SSSR, Earth Sciences Section*, **231**, 140–142.

Khanukhova, L. T., Zharikov, V. A., Ishbulatov, R. A. & Litvin, Y. A., 1977. The surface of saturation of clinopyroxenes with silica in the system CaMgSi$_2$O$_6$-NaAlSi$_2$O$_6$-CaAl$_2$SiO$_6$-SiO$_2$ at 35 kilobars and 1200 °C. *Doklady Akademii Nauk SSSR, Earth Sciences Section*, **234**, 175–179.

Klemd, R., 2003. Ultrahigh-pressure metamorphism in eclogites from the western Tianshan high-pressure belt (Xinjiang, western China) – comment. *American Mineralogist*, **88**, 1153–1156.

Kushiro, I., 1969. Clinopyroxene solid solutions formed by reactions between diopside and plagioclase. *Mineralogical Society of America Special Paper*, **2**, 179–191.

Labotka, T. C., 1995. Evidence for immiscibility in Ti-rich garnet in a calc-silicate hornfels from northeastern Minnesota. *American Mineralogist*, **80**, 1026–1030.

Liou, J. G., Zhang, R. Y., Ernst, W. G., Rumble, D. & Maruyama, S., 1998. High-pressure minerals from deeply subducted metamorphic rocks. In: *Ultrahigh-Pressure Mineralogy Reviews in Mineralogy* (ed. Hemley, R. J.), pp. 33–96. Mineralogical Society of America, Washington, DC.

Müntener, O. & Hermann, J., 1994. Titanian andradite in a metapyroxenite layer from Malenco ultramafics (Italy): implications for Ti-mobility and low oxygen fugacity. *Contributions to Mineralogy and Petrology*, **116**, 156–168.

O'Hara, M. J. & Yoder, H. S., 1967. Formation and fractionation of basic magmas at high pressures. *Scottish Journal of Geology*, **3**, 67–117.

Okamoto, K. & Maruyama, S., 2004. The eclogite-garnetite transformation in the MORB + H2O system. *Physics of the Earth and Planetary Interiors*, **146**, 283–296.

Onuma, K., Hijkata, K. & Yagi, K., 1968. Unit-cell dimensions of synthetic titan-bearing clinopyroxenes. *Journal of the Faculty of Science, Hokkaido University, Series 4*, **14**, 111–121.

Page, F. Z., Essene, E. J. & Mukasa, S. B., 2005. Quartz exsolution in clinopyroxene is not proof of ultrahigh pressures: evidence from eclogites from the Eastern Blue Ridge, Southern Appalachians U.S.A. *American Mineralogist*, **90**, 1092–1099.

Papike, J. J., 1980. Pyroxene mineralogy of the Moon and meteorites. In: *Reviews in Mineralogy, v. 7, Pyroxenes* (ed. Prewitt, C. T.), pp. 495–525, American Mineralogical Society, Washington, D.C.

Redhammer, G. J., Ohashi, H. & Roth, G, 2003, Single-crystal structure refinement of NaTiSi$_2$O$_6$ clinopyroxene at low temperatures (298 < *T* < 100K). *Acta Crystallographica*, **B59**, 730–746.

Robinson, P., 1980. The composition space of terrestrial pyroxenes – internal and external limits. In: *Reviews in Mineralogy, v. 7, Pyroxenes* (ed. Prewitt, C. T.), pp. 419–494. Mineralogical Society of America, Washington, DC.

Segnit, E. R., 1953. Some data on synthetic aluminous and other pyroxenes. *Mineralogical Magazine*, **30**, 218–226.

Sekine, T., Irifune, T., Ringwood, A. E. & Hibberson, W. O., 1986. High-pressure transformation of eclogite to garnetite in subducted oceanic-crust. *Nature*, **319**, 584–586.

Smith, D. C., 1988. In: *Eclogites and Eclogite Facies – Rocks. Developments in Petrology*. Elsevier, Amsterdam, pp. 524.

Smith, D. C., 2006, The SHAND quaternary system for evaluating the supersilicic or subsilicic crystal-chemistry of eclogite minerals, and potential new UHPM pyroxene and garnet end-members. *Mineralogy and Petrology*, **88**, 87–122

Smith, D. C. & Cheeney, R. F., 1980. Oriented needles of quartz in clinopyroxene: evidence for exsolution of SiO$_2$ from a non-stoichiometric supersilicic "clinopyroxene". 26th International Geological Congress, Paris, France, Abstracts, **1**, 145.

Smyth, J. R., 1980. Cation vacancies and the crystal-chemistry of breakdown reactions in kimberlitic omphacites. *American Mineralogist*, **65**, 1185–1191.

Sobolev, N. V., Kuznetsova, I. K. & Zyuzin, N. I., 1968. The petrology of grospydite xenoliths from the Zagad0chnaya kimberlite pipe in Yakutia. *Journal of Petrology*, **9**, 253–280.

Spear, F. S., Rumble, D. & Ferry, J. M., 1982. Linear algebraic manipulation of n-dimensional composition space. In: *Characterization of Metamorphism through Mineral Equilibria, Reviews in Mineralogy 10*, (ed. Ferry, J. M.), pp. 53–104. Mineralogical Society of America, Washington, DC.

Thompson, J. B., 1982. Reaction Space: An algebraic and geometric approach. In: *Characterization of Metamorphism through Mineral Equilibria, Reviews in Mineralogy 10* (ed. Ferry, J. M.), pp. 33–52. Mineralogical Society of America, Washington, DC.

Tsai, C. H. & Liou, J. G., 2000. Eclogite-facies relics and inferred ultrahigh-pressure metamorphism in the North Dabie Complex, central-eastern China. *American Mineralogist*, **85**, 1–8.

Tschermak, G., 1871. Ueber Pyroxen un Amphibol. *Mineralogische Mittheilungen*, **1**, 17–46.

Wang, W. Y. & Gasparik, T., 2000. Evidence for a deep-mantle origin of a NaPX-EN inclusion in diamond. *International Geology Review*, **42**, 1000–1006.

Wang, W. & Sueno, S., 1996. Discovery of a NaPx-En inclusion in diamond: possible transition zone origin. *Mineralogical Journal*, **18**, 9–16.

Wang, Q. C., Ishiwatari, A., Zhao, Z. Y. *et al.*, 1993. Coesite-bearing granulite retrograded from eclogite in Weihai, eastern China. *European Journal Of Mineralogy*, **5**, 141–151.

Williams, A. F., 1932. *The Genesis of the Diamond*, 2 volumes. Ernest Benn Limited, London.

Wood, B. J., 1979. Activity-composition relationships in Ca(Mg, Fe)Si$_2$O$_6$-CaAl$_2$SiO$_6$ clinopyroxene solid-solutions. *American Journal Of Science*, **279**, 854–875.

Wood, B. J. & Henderson, C. M. B., 1978. Compositions and unit-cell parameters of synthetic non-stoichiometric tschermakitic clinopyroxenes. *American Mineralogist*, **63**, 66–72.

Yagi, K. & Onuma, K., 1967. The join CaMg$_2$Si$_2$O$_6$–CaTiAl$_2$O$_6$ and its bearing on the titanaugites. *Journal of the Faculty of Science, Hokkaido University, series 4*, **13**, 463–483.

Zhang, L. F., Ellis, D. J. & Jiang, W., 2002. Ultrahigh-pressure metamorphism in western Tianshan, China: Part I. Evidence from inclusions of coesite pseudomorphs in garnet and from quartz exsolution lamellae in omphacite in eclogites. *American Mineralogist*, **87**, 853–860.

Zhang, L., Ellis, D., Williams, S. & Jiang, W., 2003. Ultra-high-pressure metamorphism in eclogites from the western Tianshan, China – reply. *American Mineralogist*, **88**, 1157–1160.

Zhang, L. F., Song, S. G., Liou, J. G., Ai, Y. L. & Li, X. P., 2005. Relict coesite exsolution in omphacite from Western Tianshan eclogites, China. *American Mineralogist*, **90**, 181–186.

Zvetkov, A. I., 1945. Synthesis of alumina pyroxenes and dependence of their optics on composition (in Russian with English summary). *Memoires de la Societe russe de mineralogie*, **74**, 215–222.

SUPPLEMENTARY MATERIAL

The authors have provided the following supplementary material, which is available alongside the article at http://www.blackwell-synergy.com.

Appendix S1 Criterion for excess silica (Smith & Cheeney, 1980)

Table A1. Transformation from cation basis to end-member basis. Matrix **[VCat]** contains the vectors of new end-members written in terms of the old cation components. The transformation matrix required to write mineral compositions in terms of the end-member components is **[VCat]$^{-1}$**.

Table A2. Transformation from cations to end-members in condensed oxide space. Abbreviations: quartz, (3Qtz), Ca-Ti pyroxene (CTPx), calcium Tschermak pyroxene (CaTs), kosmochlor (Ko), aegirine (Ag), hedenbergite (Hd), johannsenite (Jh), Ni-pyroxene (NiPx), enstatite (En), jadeite (Jd), and K-pyroxene (KPx). Coefficients of the condensed oxides are the sums of the appropriate rows of transformation matrix **[VCat]$^{-1}$**, as described in the text and are recast as plotting coordinates in the last three rows of the table.

Table A3. Compositions of natural pyroxene in text Fig. 3a. All analyses were recalculated on a six-oxygen basis.

Table A4. Compositions of synthetic pyroxene in text Fig. 3b.

Table A5. Singular value decomposition of the composition matrix for seven phase components in CMAS. All calculations performed using MATLAB software (Mathworks, Inc., Natick, MA, USA).

Table A6. Mass balances in CMAST.